Integrated Renewable Energy System Using High Gain Interleaved Boost Converter with Modified Cheetah Optimization Based Adaptive PI-Controller

Sharda P., Himanshu S., Pal R. K.

Department of Electrical Engineering, Medicaps University,
Indore, Madhya Pradesh, India

Abstract. This study introduces an innovative strategy to boost the uptake of Electric Vehicles (EVs) while curbing greenhouse gas emissions. Addressing the primary limitation of EVs - their reliance on energy storage - entails integrating a high-performance brushless DC (BLDC) motor renowned for its swift dynamic response and efficiency. The main objective of the study is to merge Photovoltaic (PV) energy generation with a bidirectional grid connection for powering the BLDC motor effectively. This objective is achieved by the introduction of a High Gain Interleaved Boost Converter (HGIBC) for enhancing voltage-gain ratio and system adaptability of the PV system. A novel Modified Cheetah Optimization (MCO)-based Proportional Integral (PI) controller ensures precise control signal generation for the converter. The AC supply to the motor is facilitated by a 3-phase Voltage Source Inverter (VSI), with speed regulation achieved through a PI controller. Simultaneously, the Bidirectional single phase grid augmented with an adaptive PI controller and a battery system with bidirectional converter distribute power supply to the BLDC motor fed EV during in sufficient power supply from PV system due to its ecological changes. Moreover, to validate the importance of proposed system, MATLAB/Simulink is utilized. The most important results are the proposed HGIBC exhibits a higher voltage gain when compared to other existing Boost converters and generates an increased efficiency of 97%. Also, with the optimized PI controller a steady converter output of 1000V is achieved at 0.35s which indicates a reduced settling time. Also, the proposed work generates a reduced simulation THD value of 1.21%. The significance of the obtained results lies in the delivering of high converter efficiency, improved power quality and reliable performance of BLDC motor system.
Keywords: electric vehicles, BLDC motor, photovoltaic, high gain interleaved boost converter, Modified Cheetah optimized PI controller, VSI, battery system, MATLAB/Simulink.

DOI: https://doi.org/10.52254/1857-0070.2025.2-66.03
UDC: 502.74.3

Sistem integrat de energie din surse regenerabile care folosește un convertizor de creștere intercalat cu câștig ridicat cu controler modificat bazat pe optimizarea prin metoda Ghepardului

Șarda P., Himanșu S., Pal R. K.
Universitatea Medicaps, Indore, Madhya Pradeș, India

Rezumat. Acest studiu introduce o strategie inovatoare pentru a stimula absorbția vehiculelor electrice (EVs), reducând în același timp emisiile de gaze cu efect de seră. Abordarea limitării primare a vehiculelor electrice - dependența lor de stocarea energiei - implică integrarea unui motor DC fără perii de înaltă performanță (BLDC), renumit pentru răspunsul său dinamic rapid și eficiența. Obiectivul principal al studiului este de a îmbina generarea de energie fotovoltaică (PV) cu o conexiune bidirecțională la rețea pentru alimentarea eficientă a motorului BLDC. Acest obiectiv este atins prin introducerea unui High Gain Interleaved Boost Converter (HGIBC) pentru îmbunătățirea raportului de creștere a tensiunii și a adaptabilității sistemului PV. Un nou controler Proportional Integral (PI) bazat pe Optimizarea Ghepardului Modificat (MCO) asigură generarea precisă a semnalului de control pentru convertor. Alimentarea prin curent alternativ a motorului este facilitată de un invertor de sursă de tensiune trifazat (VSI), cu reglarea vitezei realizată printr-un controler PI. Simultan, rețeaua bidirecțională monofazată, mărită cu un controler PI adaptiv și un sistem de baterii cu convertor bidirecțional, distribuie alimentarea cu energie către motorul BLDC alimentat EV în timpul unei surse de energie suficientă din sistemul fotovoltaic datorită schimbărilor sale ecologice. Mai mult, pentru a valida importanța sistemului propus, se utilizează MATLAB/Simulink. Cele mai importante rezultate sunt că HGIBC propus prezintă un câștig de tensiune mai mare în comparație cu alte convertoare Boost existente și generează o eficiență crescută de 97%. De asemenea, cu controlerul PI optimizat, se obține o ieșire constantă a convertorului de 1000 V la 0.35 s, ceea ce indică un timp de așezare redus. De asemenea, lucrarea propusă generează o valoare THD de simulare redusă de 1.21%. Semnificația rezultatelor obținute constă în furnizarea de eficiență ridicată a convertorului, calitate îmbunătățită a puterii și performanță fiabilă a sistemului de motor BLDC.

Cuvinte-cheie: vehicule electrice, motor BLDC, fotovoltaic, convertor boost interleaved cu câștig ridicat, controler PI optimizat prin metoda Ghepardului, VSI, sistem de baterii, MATLAB/Simulink.

Интегрированная система возобновляемой энергетики с использованием повышающего преобразователя с высоким коэффициентом усиления и модифицированным контроллером, оптимизированным методом Гепарда

Шарда П., Химаншу С., Пал Р.К.
Университет Медикапс, Индоре, Мадхия Прадеш, Индия

Аннотация. В этом исследовании представлена инновационная стратегия по стимулированию внедрения электромобилей (ЭМ) при одновременном сокращении выбросов парниковых газов. Устранение основного ограничения ЭМ — их зависимости от накопления энергии — влечет за собой интеграцию высокопроизводительного бесщеточного двигателя постоянного тока (BLDC), известного своим быстрым динамическим откликом и эффективностью. Основная цель исследования — объединить фотоэлектрическую (PV) генерацию энергии с двунаправленным сетевым соединением для эффективного питания двигателя BLDC. Эта цель достигается путем внедрения преобразователя с высоким коэффициентом усиления (HGIBC) для повышения коэффициента усиления напряжения и системной адаптивности фотоэлектрической системы. Новый пропорционально-интегральный (ПИ) контроллер на основе модифицированной оптимизации Cheetah (MCO) обеспечивает точную генерацию управляющего сигнала для преобразователя. Подача переменного тока на двигатель осуществляется с помощью 3-фазного инвертора напряжения (VSI), а регулировка скорости осуществляется с помощью ПИ-контроллера. Одновременно двунаправленная однофазная сеть, дополненная адаптивным ПИ-регулятором и аккумуляторной системой с двунаправленным преобразователем, распределяет электропитание на двигатель BLDC, питаемый EV, при недостаточном электропитании от фотоэлектрической системы из-за ее экологических изменений. Более того, для подтверждения важности предлагаемой системы используется MATLAB/Simulink. Наиболее важными результатами являются то, что предлагаемый HGIBC демонстрирует более высокий коэффициент усиления напряжения по сравнению с другими существующими повышающими преобразователями и генерирует повышенную эффективность 97%. Кроме того, с оптимизированным ПИ-регулятором устойчивый выход преобразователя 1000 В достигается за 0.35 с, что указывает на сокращенное время установления. Кроме того, предлагаемая работа генерирует сокращенное значение THD моделирования 1.21%. Значимость полученных результатов заключается в обеспечении высокой эффективности преобразователя, улучшенного качества электроэнергии и надежной работы системы двигателя BLDC.

Ключевые слова: электромобили, двигатель BLDC, фотоэлектрическая батарея, буст-преобразователь с высоким коэффициентом усиления, ПИ-контроллер, оптимизированный методом гепарда, VSI, аккумуляторная система, MATLAB/Simulink.

I. INTRODUCTION

The shift towards EV from Internal Combustion Engine (ICE) vehicles is driven by the need to minimize greenhouse emissions, which reduce reliance on fossil fuels [1-2]. Furthermore, by utilizing EV's various benefits like enhanced air quality, noiseless and low emissions are attained, which is crucial for meeting global environment goals [3]. The EVs propelled by BLDC motor provide a paradigm shift towards more effectual propulsion systems, which offer several advantages over conventional ICE, such as efficiency, smoother operation and minimized maintenance requirements [4-5]. Also, to further augment the ecological benefits of EVs, integrating RES such as PV system for charging becomes imperative, which harness solar energy to generate electricity without emitting greenhouse gases, which promotes the utilization of clean energy, fostering an energy ecosystem for transportation [6-7]. However, the intermittent nature of solar energy leads to voltage fluctuations that pose a challenge for EV charging [8]. To address this, DC-DC converters are essential to regulate voltage and ensure compatibility with EV charging requirements [9].

In response to the challenges of traditional converters, high gain Interleaved Boost converter emerges as a promising solution. This advanced converter topology address the challenges posed the intermittent nature of solar energy by providing improved voltage regulation, lower switching losses and minimized THD. Additionally, to ensure the converter operation for providing a stable output voltage, a controller is crucial [15].

Traditionally, Proportional Integral (PI) controller [16] have been utilized owing to their ease of implementation, simplicity and effectual performance in steady state error correction, which adjusts the converter's function to sustain a consistent voltage.

Despite their benefits, it has the limitations, particularly dealing with the dynamic and non-linear characteristics and the parameters of this controller has to be fine-tuned.
Therefore, the optimization approaches are increasingly being considered for overcoming these challenges [17-18]. The current traditional optimization methods like Particle Swarm Optimization (PSO) [19], Dragon Fly Optimization (DFO) [20] and Grey Wolf Optimization (GWO) [21] algorithms for providing optimal control parameters, enhancing system response and efficacy [22].

Table 1

Traditional Survey related to the DC-DC converter

References	Converter	Advantage	Drawbacks
SVK Naresh et al (2023) [10]	High gain Quadratic Boost converter	The extensive range voltage conversion ratio, low voltage stress and current ripples.	Though, it has three switches and requires a complicated switching scheme.
Zhengxin Liu et al (2020) [11]	High gain Boost converter	The proposed converter's highest efficiency surpasses 95% as well as the voltage ripple factor is 0.01.	However, the inductor and switching losses has to be considered in upcoming studies.
Bader et al (2022) [12]	Multiphase Interleaved Buck-Boost Converter	This converter operates in interleaved manner for high voltage gain requirements and provides quick dynamic performance.	Nevertheless, the Efficiency is dropped when the output power exceeds 310W.
Mudadla dhananjaya1 et al (2022) [13]	Multi output converter	It has the ability to provide independent regulated voltages for buck and boost topologies.	This converter has a drawbacks of high conduction losses owing to more diodes.
Subhendu Bikash Santra et al (2020) [14]	Boost converter based on a coupled inductor	This model lowers the current stress without compromising efficiency and voltage gain.	The inductance leakage and uncertainty measurement leads to disparity.

However, these topologies also have their drawbacks like it often needed significant computational resources, time to coverage to the optimal solution and high computational cost [23-24]. In order to mitigate these drawbacks, the advanced Modified Cheetah Optimization Algorithm is explored in this work, which inspired by the adaptive and swift hunting strategies of cheetahs, which dynamically adjust to changing conditions, ensuring optimal control of the converter and stable output voltage with quick convergence speed and settling time.

The contributions of the developed enhanced EV charging system are illustrated as below,

- Utilizing PV system to power BLDC motor of EV, which fosters a renewable energy ecosystem.
- The Implementation of High Gain Interleaved Boost converter offers enhanced voltage regulation, which has the ability to step up low voltage PV system to required level.
- The Modified COA-PI controller ensures optimal converter performance and stable output voltage by improving the overall efficiency of charging system.

II. PROPOSED MODELLING

The integration of RES with EV charging infrastructure is essential, which has the goal of addressing demand for clean mobility. Hence, this research focuses on the integration of RES based high gain Interleaved Boost converter with Modified Cheetah optimization algorithm specifically employing for BLDC motor technology to power EV. The block diagram is specified in Fig. 1.

The PV system generates DC power based on the available solar irradiation and environmental conditions, which is fed to high gain Interleaved Boost converter to step up PV arrays voltage to desired level. Furthermore, the PI controller is developed for stabilizing the output voltage and the Modified COA is utilized for fine tuning the PI controller parameters with quick convergence speed and settling time. The PWM generator is used for delivering pulses for superior switching operation of converter.

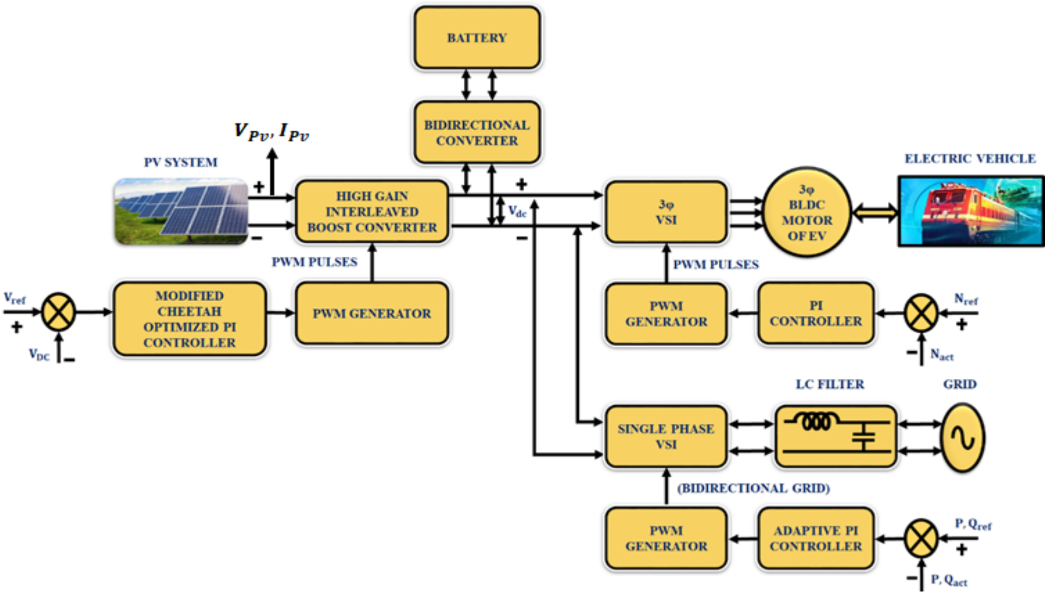

Fig. 1. Overview of PV based EV charging.

The enhanced and controlled output is fed to BLDC motor, speed of motor is regulated by PI controller. On the other hand, excess energy generated from PV system is deliver to the battery system and single phase grid through single phase VSI, which is regulated with an aid of adaptive PI controller and required pulses are formed by PWM generator for the better functioning of single phase VSI.

Moreover, the bidirectional battery converter is deployed for charging and discharging purpose as per the battery needs. During unavailable power from PV system, the BLDC motor fed EV gets powered by the battery system and bidirectional grid. Thereby, the continuous and uninterruptable power is delivered to the EV charging without any distortions.

A. Modelling of PV System

The PV system used in this study to power the BLDC motor of EV system, PV array contains multiple PV modules connected in parallel and series to meet voltage and current requirements of the BLDC motor of EV.

Moreover, it is modelled using the single-diode equivalent circuit, which includes a current source, a diode, series and parallel resistance as represents in Fig. 2.

The PV array's output current is defined as follows,

$$I = I_{sc}\left(exp\frac{q(V+R_sI}{KnT}-1\right)-\left(\frac{V+R_sI}{R_{sh}}\right) \quad (1)$$

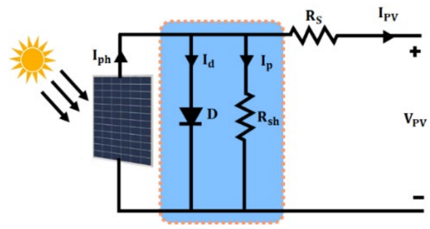

Fig. 2. Circuit diagram of PV.

Here, I_{sc} specifies the short circuit current,R_{sh} indicates shunt resistances T denotes cell temperature, K illustrates Boltzmann's constant and n refers ideal factor. Additionally, the subsequent equation (2) shows diode saturation current with respect to the temperature I_o ,

$$I_o = I_{rs}\left[\frac{T}{T_r}\right]^3 exp\left[\frac{E_{go}}{nV_t}\left(\frac{T}{T_r}-1\right)\right] \quad (2)$$

Where, I_{rs} shows the reverse saturation current, E_{go} represents band gap energy, T_r specifies the nominal temperature and V_t denotes the diode thermal voltage of solar PV cell correspondingly.

The voltage generated by PV is low because it is affected by ecological factors, thus it necessitates the usage of high gain Interleaved Boost converter to enhance the gain at output, which is discussed elaborately in below section.

B. Modelling of High Gain Interleaved Boost Converter

The HGIBC, which has advantages over typical boost converters like lower output ripple current, lower THD, and higher voltage, is one viable way to boost PV system's low voltage output. The developed HGIBC has 2 switches, 4 diodes, 4 capacitors and 2 inductors as specified in Fig. 3, also it operated in three modes with respect to the ON/OFF condition as represented in Fig. 4 and is explained as follows.

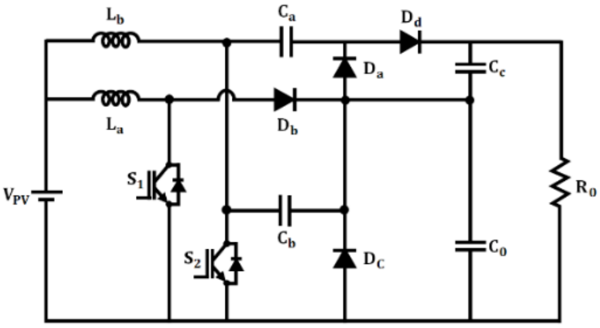

Fig. 3. Circuit diagram of proposed HGIBC.

Mode 1 of HGIBC: In this condition, all the four diodes are in reversed biased during the switches S_1 and S_2 is in the conduction mode. The respective path for current flow is displayed in Fig. 4(a), which shows that the PV system is currently charging the L_1 and L_2 as well as it gradually raised. Furthermore, the output capacitors C_c and C_o are linked in series to deliver power to the load.

Mode 2 of HGIBC: During S_1 turned OFF and S_2 is in ON condition, D_a and D_c are the only diodes are in conducting. The appropriate flow for the current is depicted in Fig. 4(b), which indicates that since L_a is still being charged at this moment and rising the inductor current and C_a gets charged by the PV system. The energy is transmitted to C_o and the load when the PV, L_b and C_b are linked in series. The capacitor C_c discharges energy to the load, which lowers the inductor current on L_b .

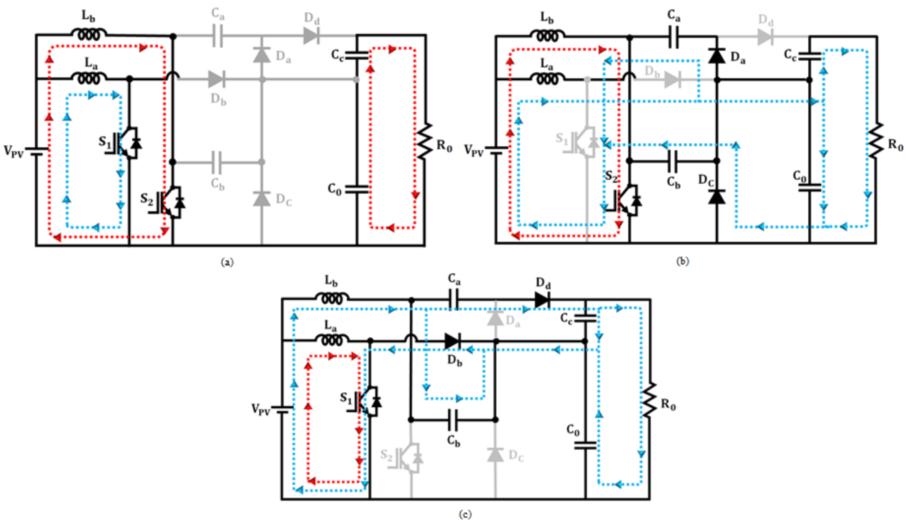

Fig.4. HGIBC (a) Mode 1 (b) Mode 2 and (c) Mode 3.

Mode 3 of HGIBC: In this state, the diodes D_b and D_d are in conduction when S_2 in OFF state and the corresponding path of current flow is illustrated in Fig. 4(c), L_a is still charged at this moment, which rising inductor's current and C_b gets charged by the PV system. Moreover, the energy is deliver to load and capacitor C_o by a series connection over PV, L_a and C_a at the same time, C_o discharges energy to load, which lowers the inductor current on L_a.

The switching waveform for the HGIBC is represented in Fig. 5. By utilizing the volt second balance principle, and voltage gain is examined, during switch S_1 is in OFF condition for the inductance L_a,

$$V^I{}_{La} \cdot T_{1on} = V^{II}{}_{La} \cdot T_{1off} \tag{3}$$

Here, turn ON and OFF time of switch S_1 is represented by T_{1on} and T_{1off} correspondingly.

V_{La} is expressed as follows using Mode 1 and 2 equivalent circuit of HGIBC,

$$V^I{}_{La} = V_{PV} \tag{4}$$

By using equations (3) and (4),

$$V^{II}{}_{La} = \frac{T_{1on}}{T_{1off}} \cdot V^I{}_{La} = \frac{D_a}{1-D_a} \cdot V^I{}_{La} = \frac{D_a}{1-D_a} \cdot V_{PV} \tag{5}$$

Where, $D_a = \frac{T_{1on}}{T_{1on+T_{1off}}}$ = duty cycle of S_1.

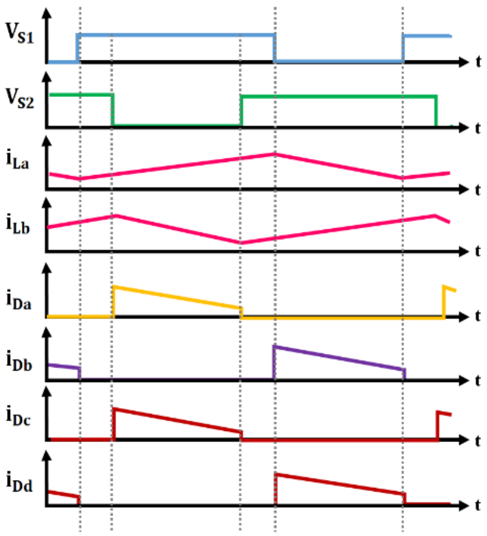

Fig. 5. Switching waveform for the developed HGIBC.

During switch S_1 is in OFF condition for the inductance L_b,

$$V^I{}_{Lb} \cdot T_{2on} = V^{II}{}_{Lb} \cdot T_{2off} \tag{6}$$

V_{Lb} is expressed as follows using Mode 1 and 2,

$$V^I{}_{Lb} = V_{PV} \tag{7}$$

By using equations (6) and (7),

$$V^{II}{}_{Lb} = \frac{T_{2on}}{T_{2off}} \cdot V^I{}_{Lb} = \frac{D_b}{1-D_b} \cdot V^I{}_{La} = \frac{D_b}{1-D_b} \cdot V_{PV} \tag{8}$$

Where, $D_b = \frac{T_{2on}}{T_{2on+T_{2off}}}$ = duty cycle of S_2

Equations (9 and 10) represents the Mode 2 and 3 voltage on C_a and C_b obtained,

$$V_{Ca} = V_{PV} + V^{II}{}_{Lb} = V_{PV} + \frac{D_b}{1-D_b} \cdot V_{PV} = \frac{1}{1-D_b} \cdot V_{PV} \tag{9}$$

$$V_{Cb} = V_{PV} + V^{II}{}_{Lb} = V_{PV} + \frac{D_a}{1-D_a} \cdot V_{PV} = \frac{1}{1-D_a} \cdot V_{PV} \tag{10}$$

Concurrently, from mode 3 and 2 the obtained voltage on C_c and C_o is expressed in the subsequent equation (11 and 12),

$$V_{Cc} = V_{PV} + V^{II}{}_{La} + V_{Ca} = V_{PV} + \frac{D_a}{1-D_a} \cdot V_{PV} = \frac{1}{1-D_b} \cdot V_{PV} \tag{11}$$

$$V_{Co} = V_{PV} + V^{II}{}_{Lb} + V_{Cb} = V_{PV} + \frac{D_b}{1-D_b} \cdot V_{PV} = \frac{1}{1-D_a} \cdot V_{PV} \tag{12}$$

The voltage in C_c and C_o equations is illustrated in below equation (13) by assuming the equal duty ratios ($D_a = D_b = D$),

$$V_{Cc} = V_{Co} = \frac{2}{1-D} \cdot V_{PV} \tag{13}$$

The developed HGIBC is expressed by the below equation from Mode 1 and 2,

$$V_o = V_{Cc} + V_{Co} \tag{14}$$

The output of HGIBC is illustrated by applying equation (13 and 14) as follows,

$$V_o = \frac{4}{1-D} \cdot V_{PV} \tag{15}$$

Here, V_{Out}/V_{in} is the voltage gain of the developed converter is expressed as follows by utilizing equation (11),

$$\text{Voltage gain of HGIBC} = \frac{V_o}{V_{PV}} = \frac{4}{1-D} \tag{16}$$

By adopting this HGIBC, the high voltage gain with reduced power losses are obtained, also the subsequent Modified Cheetah Optimization Algorithm is developed for fine tuning the parameters of the PI controller by providing stable output voltage and desired control performance that is discussed in detailed.

C. Modelling of Modified Cheetah Optimization Algorithm

The PI controller is normally employed to regulate the converter operation for obtaining better performance and the optimization approach is crucial for tuning this control parameter under varying operating conditions. Thus, the MCOA is proposed in this work, which is an advanced metaheuristic approach inspired by the hunting strategies of cheetahs, which designed to solve complex optimization issues with improved efficiency and accuracy. This algorithm mimics the cheetah's speed, agility and strategy in hunting. Conventional CO algorithm has better abilities in solving large scale issues. Nonetheless, it required enhancement in the convergence rate and settling time for defining the parameters of PI controller. Henceforth, for overcoming such issues the Modified type of CO algorithm is introduced. The algorithm functions on the principle that the optimal solution is identified by the best position within the population, similar to how cheetahs identify their prey. The cheetahs adjust their hunting strategies to enhance their success over the course of their hunt, thereby the MCOA efficiently finds for optimal solutions to complex issues. The proposed algorithm integrates the entirety of the hunting procedure, strategically deploying these tactics over various hunting cycles or iterations. Essentially, COA leverages these astute hunting behaviour iteratively throughout its hunting process as illustrated in Fig. 6.

Searching: In the searching phase, cheetahs actively scan their territories or the surrounding areas to locate prey with in their search space.

Sitting and Waiting: During the sitting and waiting phase, cheetahs selects to remain stationary upon detecting prey, especially under unfavorable conditions. This strategy allows the cheetah to conserve energy and wait for the prey to approach closer for a more opportune moment to initiate the hunt.

Attacking: the Cheetahs sprint over the prey at high speed once it start to attack and capture the prey by closing in rapidly.

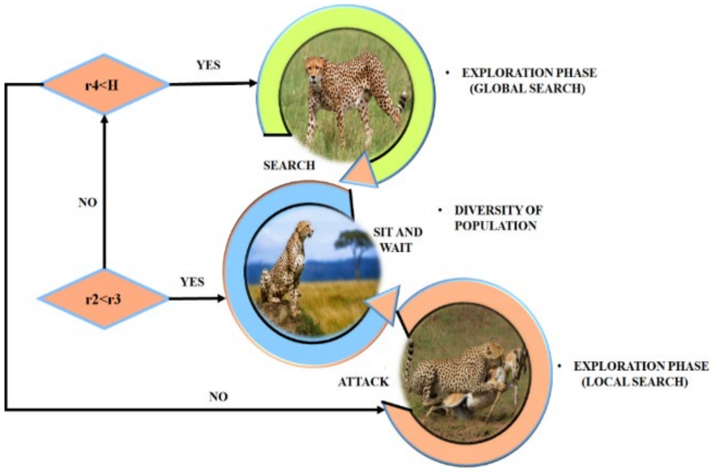

Fig. 6. MCO's Algorithm strategy selection mechanism.

Searching Strategy: In search mode, equation (17) is given as follows,

$$X^{i+1}_{i,j} = X^{i}_{L,j} + \hat{r}^{t} \,.\, \alpha^{t}_{i,j} \tag{17}$$

Here, the modified random length $\alpha^{t}_{i,j}$ and parameter $\hat{r}^{t}$ is expressed as below,

$$\hat{r}^{t} = r'/r'' \tag{18}$$

$$\alpha^{t}_{i,j} = X^{t}_{k',j} - X^{t}_{i',j} \tag{19}$$

Where, $X^{t}_{k',j}$ and $X^{t}_{i',j}$ are denoted as positions of ith and kth cheetahs in the sorted population r' and r'' specifies the normal random values of distribution Function.

Fig. 7 denotes the flowchart of modified COA. The local search phase is enhanced by updating each cheetah's position in relation to the group leader's position. Additionally, equation (18) shows variation in the responses, which aids in the phase of global search. The random parameter, by producing long steps during the hunting period, extends the solution beyond the range of variables, resulting the replacement of the out of range solution with a new random solution in population, also it avoid an algorithm from getting stuck in local optima.

Attacking Strategy: The reformulated of the attacking strategy of Modified COA is illustrated as below.

$$X^{i+1}_{i,j} = X^{i}_{B,j} + \hat{r}^{t} .\ \beta^{t}_{i,j} \qquad (20)$$

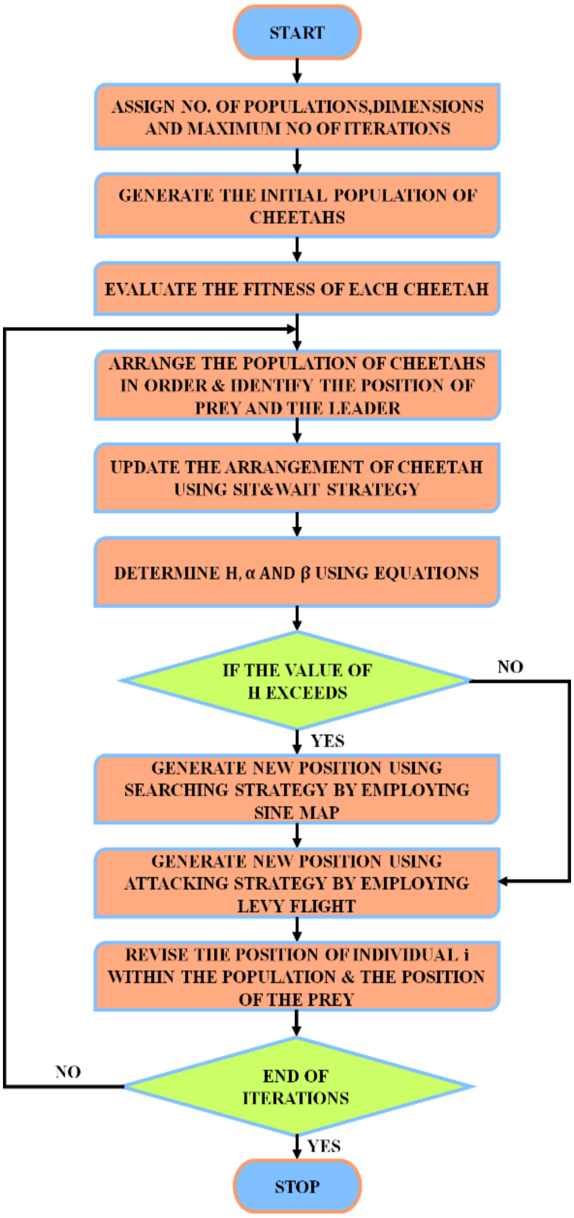

Fig. 7. Flowchart of the developed Modified COA.

Here, the random value in a range of [0, 1] denoted as $\hat{r}^{t}$ p. The interaction factor is demonstrated by the proximity to neighboring cheetahs as indicates in Equation (19) in the MCOA. Typically, the cheetahs pursue their prey independently, their positions has to be adapted relative to the prey's location. Thus, cheetah modifies its position in relation to the prey at attack phase and is,

$$\beta^{t}_{i,j} = X^{i}_{B,j} - X^{t}_{i,j} \qquad (21)$$

The faster near optimal solution is determined with the assistance of the developed attack strategy. Henceforth, the MCOA's exploitation phase is efficiently enhanced with its high convergence speed. Moreover, the enhanced and stabilized output voltage is deliver to three phase BLDC Motor through the VSI.

D. Modelling of Three Phase BLDC Motor

It is a type of synchronous electric motor that operates on DC, which uses an electronic communication system to control the flow of windings. This results in various advantages like higher efficiency and better speed torque with longer lifespan. The operating principle of this motor revolves around a permanent magnet motor and a stator with windings. This process generates the back EMF in the windings to determine the rotor position and maintains the synchronization over the stator and rotor. Fig. 8 indicates the equivalent circuit and mechanical model of BLDC motor. The following equation (20) illustrates the BLDC dynamic model,

$$\begin{bmatrix} V_a \\ V_b \\ V_c \end{bmatrix} = \begin{bmatrix} r_s & 0 & 0 \\ 0 & r_s & 0 \\ 0 & 0 & r_s \end{bmatrix} + S \begin{bmatrix} L & M & M \\ M & L & M \\ M & M & L \end{bmatrix} + \begin{bmatrix} e_a \\ e_b \\ e_c \end{bmatrix} \qquad (22)$$

Here, V specifies the phase voltage, S indicates the Laplace operator, M denotes the mutual inductance over the phases and L represents the self-inductance respectively.

$$i_a + i_b + i_c = 0 \qquad (23)$$

$$Mi_b + Mi_c = -Mi_c \qquad (24)$$

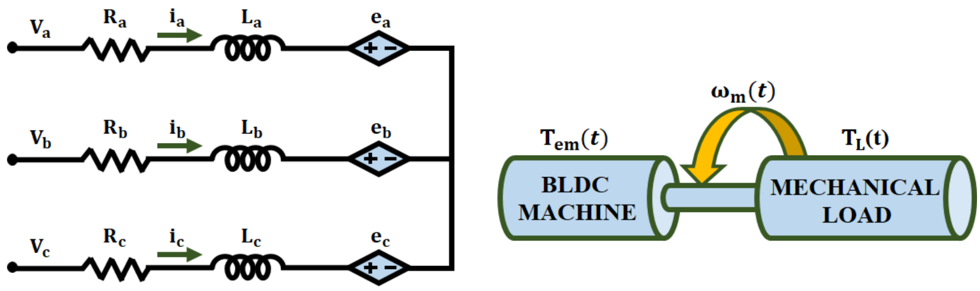

Fig. 8. Equivalent circuit and the mechanical model of BLDC motor.

By applying equation (22) in (20), is expressed as follows,

$$L_s = L\begin{bmatrix} \frac{di_a}{dt} \\ \frac{di_b}{dt} \\ \frac{di_c}{dt} \end{bmatrix} = \begin{bmatrix} 1 & 0 & 0 \\ 0 & 1 & 0 \\ 0 & 0 & 1 \end{bmatrix}\begin{bmatrix} V_{an} \\ V_{bn} \\ V_{cn} \end{bmatrix} - \begin{bmatrix} r_s & 0 & 0 \\ 0 & r_s & 0 \\ 0 & 0 & r_s \end{bmatrix}\begin{bmatrix} i_a \\ i_b \\ i_c \end{bmatrix} - \begin{bmatrix} e_a \\ e_b \\ e_c \end{bmatrix} \tag{25}$$

The following equation (24) defines the torque as,

$$T_e = \left[\frac{P}{2}\right]\frac{e_a i_a + e_b i_b + e_c i_c}{\omega_m} \tag{26}$$

Here ω_m indicates the rotation speed of the motor. Furthermore, the motor control is done by the PI controller for regulating the speed. Battery is employed for storing surplus energy obtained from the PV system.

The extra energy is transmitted into the grid system through the single VSI, just as before, after supplying the BLDC motor fed EV with sufficient power.

The stored energy from the battery and grid are deliver power to the motor during the unavailable power from PV system. Also, to control single phase VSI, the adaptive PI controller is used for grid synchronization as explained below.

E. Modelling of Adaptive PI Controller

An adaptive PI controller automatically adjusts its proportional and integral (PI) parameters to regulate the VSI. Traditional PI controllers often rely on fixed gains which are not optimal under varying operating conditions.

In contrast, adaptive PI controller automatically adjusts its parameters based on real-time variations in system conditions, thereby improving response time, stability and overall performance. The traditional PI controller contains two gains such as K_p and K_i the updated traditional PI to be adaptive as demonstrated in equation (28-31),

$$C(s) = K_p + \left(K_i/s\right) \tag{27}$$

$$output(t) = -K_c(error*error + \int_0^t error*error\ dt) \tag{28}$$

Here, K_p, K_i and K_c represents the proportional gain, Integral gain, Constant gain with error signal.

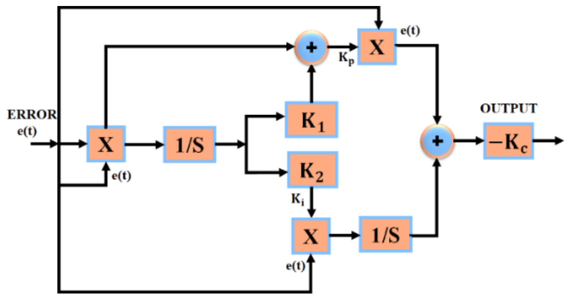

Fig. 9. Representation of Adaptive PI controller.

$$K_p = error*error + K_1\int_0^t error*error\ dt \tag{29}$$

$$K_i = K_2\int_0^t error*error\,dt \tag{30}$$

Here, K_1 and K_2 indicates the parameters of adaptive initialization and Fig.9 represents the Adaptive PI controller. The adaptive initialization parameters assure that the controller refines its response to system variations in a dynamic manner. This reduces the steady-state error and improves transient performance. The system output is continuously monitored by the controller and the error signal is calculated. This error denotes the deviation from the desired reference value. The PI gains are updated using the adaptive equations based on real-time error and its rate of change. Finally, the controlled and continuous power supply is distributed to the three phase BLDC motor fed EV system without any disturbances.

The parameters are continuously refined by the controller for maintaining optimal motor performance under varying environmental and load conditions. With the adopting of adaptive PI controller, precise control over voltage regulation is attained along with reduced THD and enhanced power quality.

III. RESULTS AND DISCUSSION

The overall outcomes for the proposed HGIBC with Modified COA obtain from the MATLAB/Simulink are elaborated. The parameter specification for the proposed work is presented in Table 2, which is given as follows.

Fig. 10 represents the solar panel waveform for this proposed work, which observed in Fig. 10(a), the temperature of solar gets deviated few seconds and after 0.25s it maintains stable voltage at 35°C.

Similarly, the intensity waveform as shown in Fig. 10(b) specifies that the intensity is constantly stable at 1000(W/Sq.m) after facing slight fluctuations.

Table 2

Parameter Specification

Parameter	Description
Solar PV System	
Open circuit Voltage	$37.25V$
Short circuit Current	$8.95A$
Series Connected solar PV cell	4
Parallel Connected solar PV cell	8
Maximum power Voltage	$29.95V$
Maximum Current	$8.35A$
High gain Interleaved Boost converter	
Switching Frequency	$10\ kHz$
$C_{1,}, C_2, C_3, C_4$	$22\ \mu F$
L_a, L_b	$1.1\ mH$

Case 1 – Varying Temperature Varying Intensity

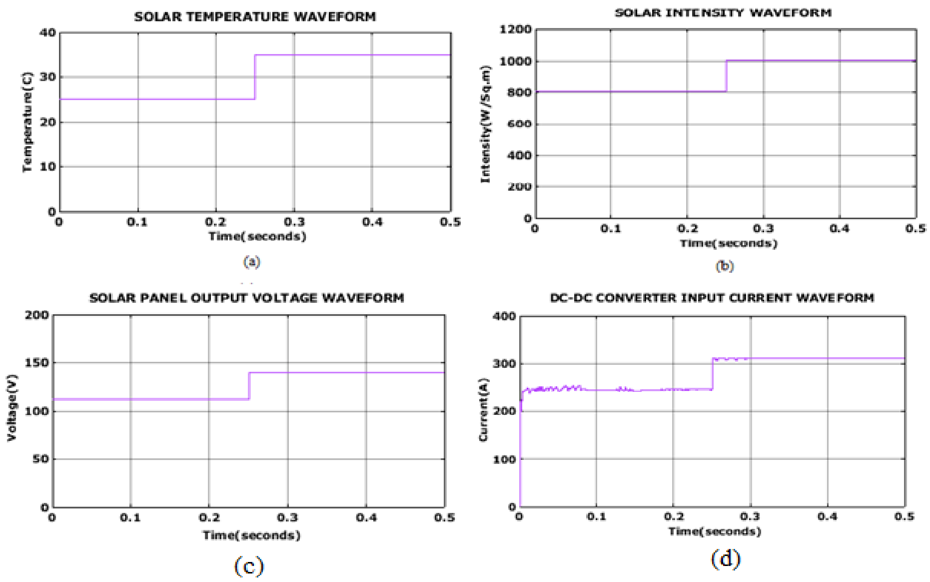

Fig. 10. Solar panel Waveform (a) Temperature (b) Intensity (C) Output voltage and (d) Input current for case 1.

Likewise, the voltage of solar panel output varies slightly in initial time as in Fig. 10(c) and after 0.25s it gradually stabilized at 140V respectively. From the current waveform it is evident that the input current highly oscillated during initial periods and after 0.35s the constant current is maintained at 310A as indicates in Fig. 10(d).

The converter output voltage for the developed converter has gained the stable voltage at 1000V after 0.45s by utilizing the PI controller as represents in Fig. 11(a). Similarly, the output voltage gets stabilized at 1000V with rapid settling time of 0.35s as presented in Fig. 11(b). The converter output current waveform using PI controller is indicated in Fig. 11(c) shows that the current gets oscillates highly in initial period after 0.4s it maintained stabilized voltage of 40A respectively. Fig. 11 (d) denotes the output current using MCO-PI controller. Fig. 11(e) represents the combined outputs attained using both controllers.

The battery waveform in Fig. 12 indicates 80% as specified in Fig. 12(a). The battery current waveform indicated in Fig. 12(b) demonstrates that the current gets deviated certain period in initial time and after 0.4s it maintains. As shown in Fig. 12(c), voltage of the battery gets stabled after 0.05s at 245V correspondingly.

Fig. 15 shows grid voltage and current waveform, from the graph it is evident that a grid voltage gets maintained constantly at 400 and similarly the current gradually constant at 12A correspondingly.

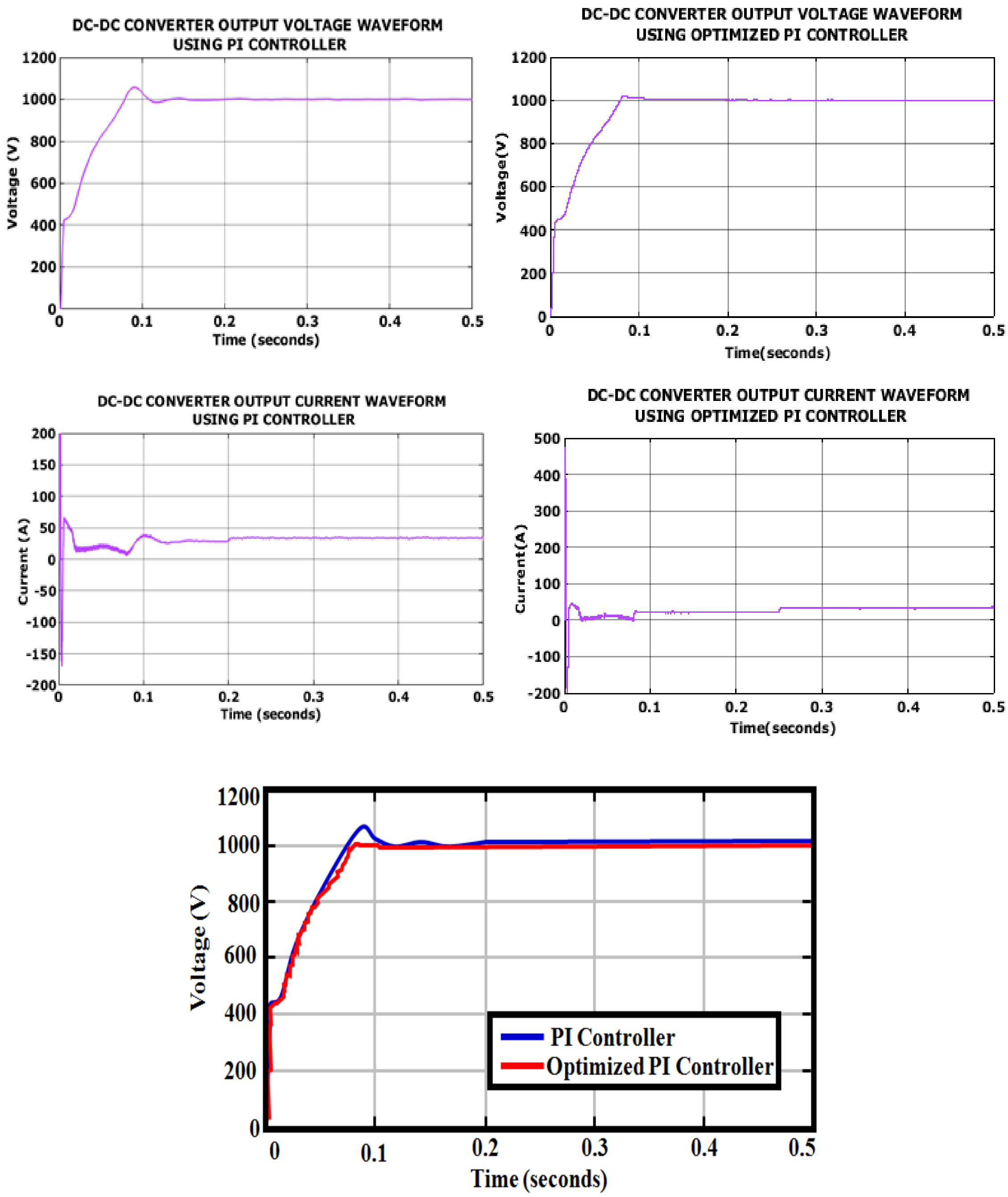

Fig. 11. Converter waveform (a) PI Output Voltage (b) Output voltage using MCO-PI controller (c) Output current using PI controller (d) Output current using MCO-PI controller (e) Combined output.

Fig. 13 illustrates the grid voltage waveform, which observed that the grid voltage gets maintained at 400V without any oscillations. Moreover, the grid current waveform specified in Fig. 14 shows that the current attains stabilized at 12A.

A. Constant speed 2000RPM under 1.5NM and 2NM load condition

After the application of a 1.5 Nm load, the motor shows minor fluctuations but successfully stabilizes at 2000 RPM within 0.02s, ensuring consistent operation under the increased load. Also, motor torque rises during the transient state and stabilizes at 1.5 Nm, equal to the applied load, confirming the motor's effective load-handling capability. As illustrated in Figure 16 motor initially responds with a slight speed fluctuation and rapidly stabilizes at the target speed of 2000 RPM, maintaining performance under the higher load. Likewise, motor torque rises proportionally to the load and stabilizes at 2 Nm, demonstrating its ability to sustain heavier loads without compromising speed.

The proposed HGIBC THD is illustrated in Fig. 17, analyzed that the developed work attains the THD value of 1.21% respectively.

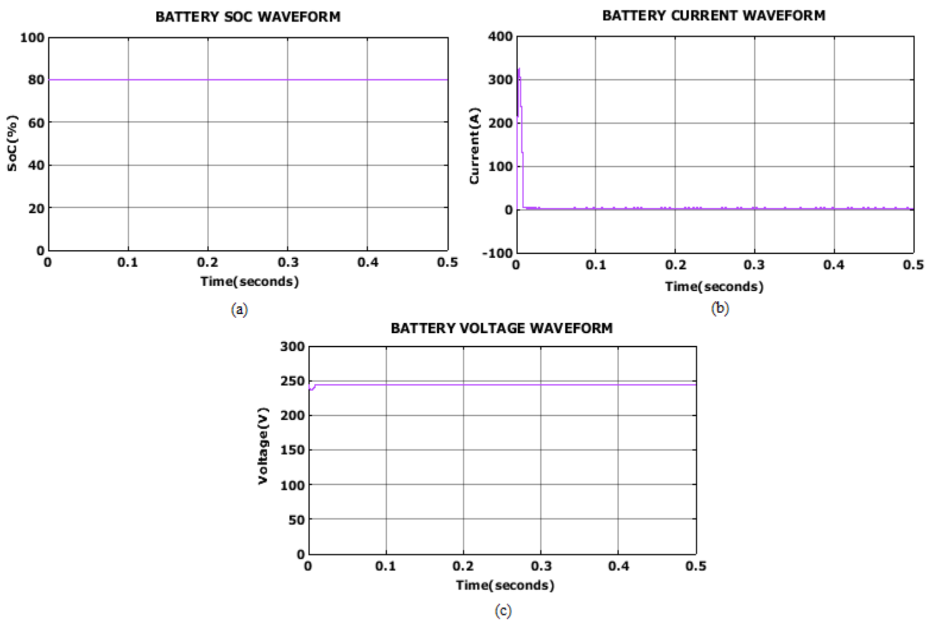

Fig. 12. Battery waveform (a) SOC (b) Current and (c) Voltage.

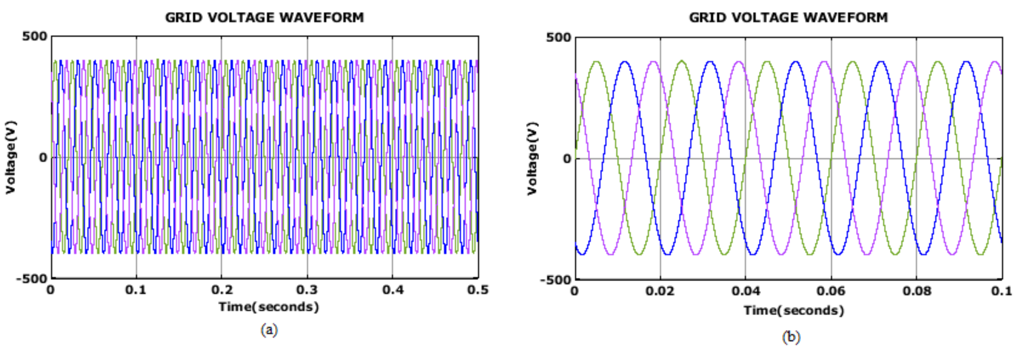

Fig. 13. Grid voltage waveform (a) Normal View and (b) Zoomed view.

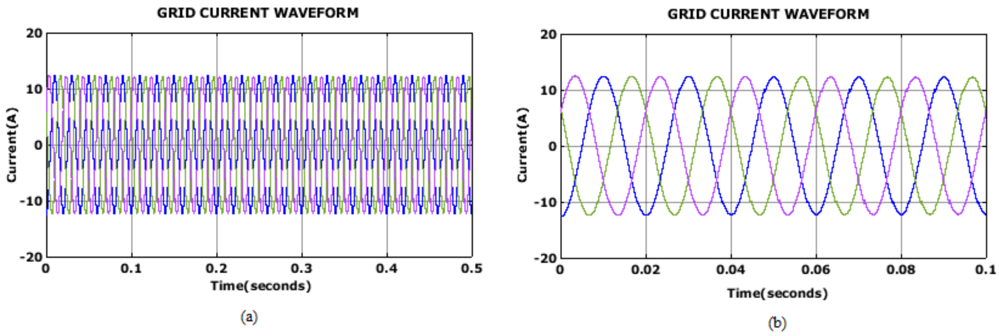

Fig. 14. Grid current waveform (a) Normal view and (b) Zoomed view.

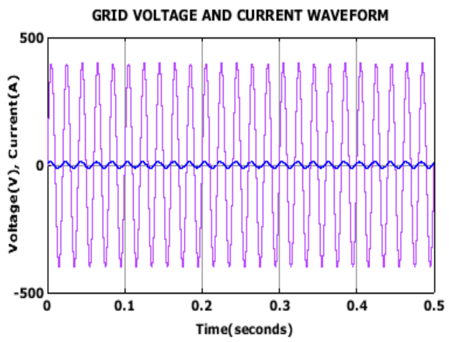

Fig. 15. Grid voltage and current waveform.

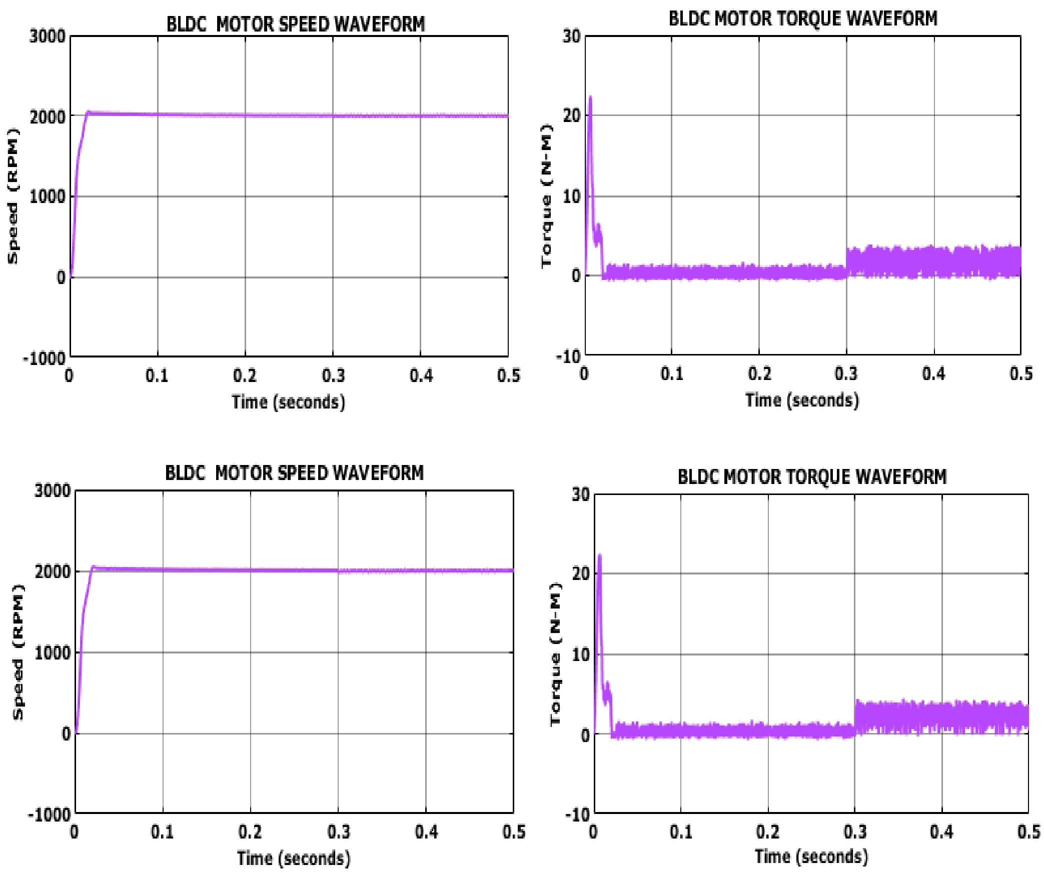

Fig. 16 BLDC motor waveforms under Constant speed 2000RPM under 1.5NM and 2NM load condition.

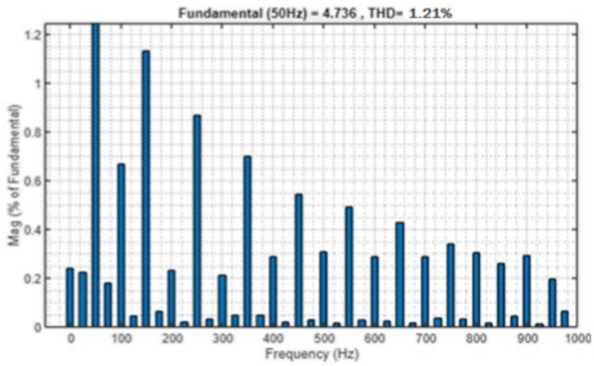

Fig. 17. THD output.

The comparison of proposed HGIBC with traditional converter is exemplified in Fig.18, from the above graph it is obvious that developed converter has high voltage gain ratio compared to traditional boost converter. The comparison graph for the efficiency of the developed work, which analyzed that the proposed HGIBC with optimized MCO-PI controller attains superior efficiency of 97% compared to traditional converter with optimized control approaches as referred in [29-31] as illustrated in Fig. 19.

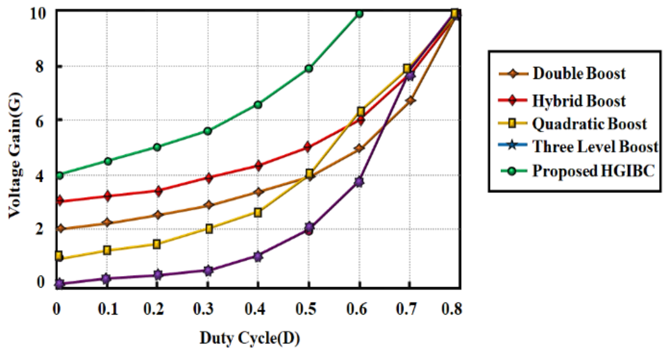

Fig. 18. Comparison of Voltage gain for various converter.

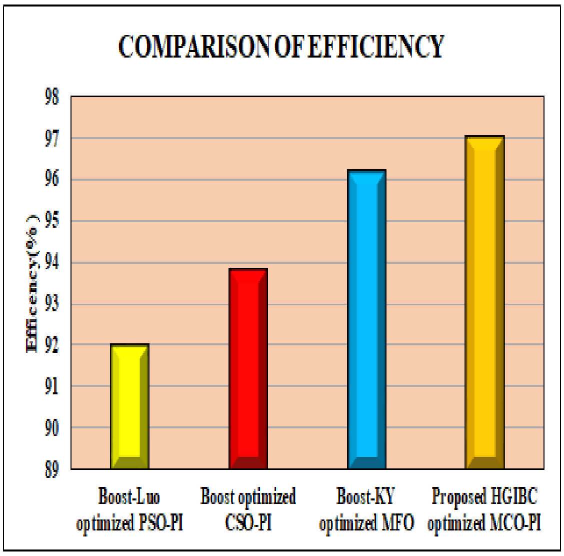

Fig. 19. Comparison of converter Efficiency

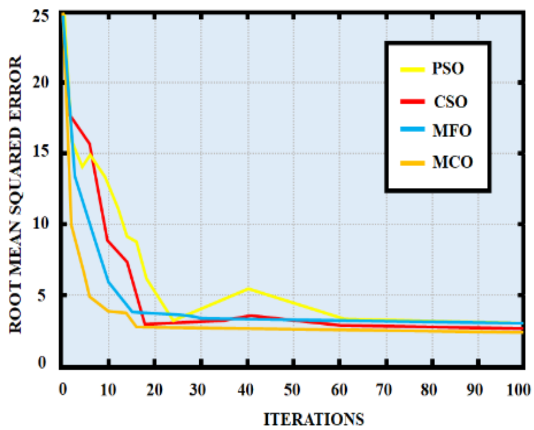

Fig. 20. Comparison of optimization approaches.

The comparison graph for the optimization approaches are exemplified in Fig. 20, which obvious that the developed MCO algorithm achieves minimized RMSE compared to the other conventional optimization approaches respectively.

IV. CONCLUSION

The proposed work presents the integration of RES with a HGIBC based MCOA optimized PI controller for powering BLDC motor fed EVs. This approach not only improves the performance and reliability of EVs by ensuring stable and optimized power supply but also promotes the adoption of RES such as PV, thereby decreasing dependence on fossil fuels and minimizing greenhouse gas emissions. The HGIBC delivers high amount of power to the required level of BLDC motor with high voltage gain and reduced power losses. Subsequently, by employing the MCOA the stabilized output is gained with rapid convergence speed and overall enhanced efficiency. On the other hand, during insufficient power from the PV system, the BLDC motor fed EV runs with the aid of battery and bidirectional single phase grid system. The proposed work is applied in MATLAB/Simulink and the comparative analysis proves that the developed converter and optimized control technique accomplishes high voltage gain, minimized THD (1.21%), efficiency (97%) with less settling time. Thereby, this work contributes significantly to the eco-friendly EV solutions by offering a superior path over a cleaner and ecological friendly future.

REFERENCES

[1] Ravi S.S, Brace C., Larkin C., Aziz M., Leach F., WG Turner J. On the pursuit of emissions-free clean mobility–Electric vehicles versus e-fuels. *Science of the Total Environment*, 2023, vol. 875, pp. 162-688.

[2] Gautam A.K., Tariq M., Pandey J. P., Shankar Verma K., Urooj S. Hybrid sources powered electric vehicle configuration and integrated optimal power management strategy. *IEEE Access*, 2022, vol. 10, pp. 121684-121711.

[3] Ahmed I., Rehan M., Basit A., Tufail M., Hong K.S. Neuro-fuzzy and networks-based data driven model for multi-charging scenarios of plug-in-electric vehicles. *IEEE Access*, 2023.

[4] Bala Murali Krishna V., Vuddanti S. Identification of the best topology of delta configured three phase induction generator for distributed generation through experimental investigations. *International Journal of Emerging Electric Power Systems*, 2022, vol. 23, no. 3, pp. 329-341.

[5] Bharathi M.L. Extraction of maximum power from solar with BLDC motor driven electric vehicles based HHO algorithm. *Advances in Engineering Software*, 2022, vol. 170, pp. 103137.

[6] Radhakrishnan R.K.G, Marimuthu U., Balachandran P.K., Mohd Shukry A.M., Senjyu T. An intensified marine predator algorithm (MPA) for designing a solar-powered BLDC motor used in EV systems. *Sustainability*, 2022, vol. 14, no. 21, pp. 14120.

[7] Gautam A.K., Tariq M., Shankar Verma K., Prakash Pandey J. An intelligent BWO algorithm-based maximum power extraction from solar-PV-powered BLDC motor-driven light electric vehicles. *Journal of Intelligent & Fuzzy Systems*, 2022, vol. 42, no. 2, pp. 767-777.

[8] Benavides D., Arévalo P., Villa-Ávila E., Aguado J.A., Jurado F. Predictive power fluctuation mitigation in grid-connected PV systems with rapid response to EV charging stations. *Journal of Energy Storage*, 2024, vol. 86, pp. 111230.

[9] Mukherjee S., Ruiz J.M., Barbosa P. "A high power density wide range DC–DC converter for universal electric vehicle charging. *IEEE Transactions on Power Electronics*, 2022, vol. 38, no. 2, pp. 1998-2012.

[10] Naresh S.V.K, Peddapati S., Alghaythi M.L. A novel high quadratic gain boost converter for fuel cell electric vehicle applications. *IEEE Journal of Emerging and Selected Topics in Industrial Electronics*, 2023, vol. 4, no. 2, pp. 637-647.

[11] Liu Z., Du J., Yu B. Design method of double-boost DC/DC converter with high voltage gain for electric vehicles. *World Electric Vehicle Journal,* 2020, vol. 11, no. 4, pp. 64.

[12] Alajmi B.N, Marei M.I., Abdelsalam I., Ahmed N.A. Multiphase interleaved converter based on cascaded non-inverting buck-boost converter. *IEEE Access*, 2022, vol. 10, pp. 42497-42506.

[13] Dhananjaya M., Ponuru D., Babu T.S., Aljafari B., Alhelou H.H. A new multi-output DC-DC converter for electric vehicle application. *IEEE access*, 2022, vol. 10, pp. 19072-19082.

[14] Santra S.B., Chatterjee D., Siwakoti Y.P., Blaabjerg F. Generalized switch current stress reduction technique for coupled-inductor-based single-switch high step-up boost converter. *IEEE Journal of Emerging and Selected Topics in Power Electronics*, 2020, vol. 9, no. 2, pp. 1863-1875.

[15] Prem P., Sivaraman P., Sakthi Suriya Raj J.S., Jagabar Sathik M., Almakhles D. Fast charging converter and control algorithm for solar PV battery and electrical grid integrated electric vehicle charging station. *Automatika: časopis za automatiku, mjerenje, elektroniku, računarstvo i komunikacije*, 2020, vol. 61, no. 4, pp. 614-625.

[16] Zellouma D., Bekakra Y., Benbouhenni H. Field-oriented control based on parallel proportional–integral controllers of induction motor drive. Energy Reports, 2023, vol. 9, pp. 4846-4860.

[17] Razmjooy N., Vahedi Z., Estrela V.V., Padilha R., Borges Monteiro A.C. Speed control of a DC motor using PID controller based on improved whale optimization algorithm. *In Metaheuristics*

and Optimization in Computer and Electrical Engineering, 2020, pp. 153-167. Cham: Springer International Publishing.

[18] Femi R., Sree Renga Raja T., Shenbagalakshmi R. Performance comparison of optimization algorithm tuned PID controllers in positive output Re-lift Luo converter operation for electric vehicle applications. *IETE Journal of Research*, 2023, vol. 69, no. 12, pp. 9394-9412.

[19] Sadeghi D., Naghshbandy A.H., Bahramara S. Optimal sizing of hybrid renewable energy systems in presence of electric vehicles using multi-objective particle swarm optimization. *Energy*, 2020, vol. 209, pp. 118471.

[20] Li S., Chu L., Hu J., Pu S., Li J., Hou Z., Sun Z. A Novel A-ECMS Energy Management Strategy Based on Dragonfly Algorithm for Plug-in FCEVs. *Sensors,* 2023, vol. 23, no. 3, pp. 1192.

[21] Padhy S., Panda S. Application of a simplified Grey Wolf optimization technique for adaptive fuzzy PID controller design for frequency regulation of a distributed power generation system. *Protection and Control of Modern Power Systems*, 2021, vol. 6, no. 1, pp. 1-16.

[22] Kancherla A.B., Bhanu Prasad N., Ravi Kishore D. PV-Based Grid Integrated EV with GWO Optimized PI Controller for Boost Integrated Luo Converter. *Journal of the Institution of Engineers (India): Series B*, 2024, vol. 105, no. 2, pp. 309-321.

[23] Shi L., Zhan Z., Liang D., Zhang J. Memory-based ant colony system approach for multi-source data associated dynamic electric vehicle dispatch optimization. *IEEE Transactions on Intelligent Transportation Systems*, 2022, vol. 23, no. 10, pp. 17491-17505.

[24] Das R., Wang Y., Busawon K., Putrus G., Neaimeh M. Real-time multi-objective optimisation for electric vehicle charging management. *Journal of Cleaner Production*, 2021, vol. 292, pp. 126066.

[25] Chakravarthi B. N., Siva Krishna Rao G.V. A high gain novel double-boost converter for DC microgrid applications. *Journal of Circuits, Systems and Computers,* 2020, vol. 29, no. 15, pp. 2050246.

[26] Valdez-Resendiz J.E., Rosas- Caro J.C., Mayo-Maldonado J.C., Llamas-Terres A. Quadratic boost converter based on stackable switching stages. *IET Power Electronics*, 2018, vol. 11, no. 8, pp. 1373-1381.

[27] Gu Y., Chen Y., Zhang B., Qiu D., Xie F. High step-up DC–DC converter with active switched LC-network for photovoltaic systems. *IEEE Transactions on Energy Conversion*, 2018, vol. 34, no. 1, pp. 321-329.

[28] Rezaie M., Abbasi V. Effective combination of quadratic boost converter with voltage multiplier cell to increase voltage gain. *IET Power Electronics*, 2020, vol. 13, no. 11, pp. 2322-2333.

[29] Vijayarangan V.A., Kaliyaperumal S. Design of Boost Integrated Luo Converter for Grid Tied EV Based Charging Station. *International Journal of*

[30] *Electrical and Electronics Research*, 2023, vol. 11, no. 4, pp. 1167-1175.

[31] Mariprasath T., Hussaian Basha C.H., Khan B., Ali A. A novel on high voltage gain boost converter with cuckoo search optimization based MPPT Controller for solar PV system. *Scientific Reports*, 2024, vol. 14, no. 1, pp. 8545.

[32] Gadekar S.D., Murali M. Optimizing Electric Vehicle Charging with Moth Flame Control Algorithm of Boost-KY Converter. Problemele Energeticii Regionale, 2023, vol. 60, no. 4, pp. 126-140.

Information about authors.

Sharda Patwa, Research Scholar in the Medicaps University Indore Madhya Pradesh. Her research interests include Electrical Power systems, Renewable Energy and Electrical machines/Drives. Email: shardapatwa82@gmail.com

Ram Kishore Pal is currently working in Medicaps University, Indore. Area of research are power system protection. Email: ramkishore.pal@medicaps.ac.in

Himanshu Shekhar is currently working in Medicaps University, Indore. Area of research are power system protection and automatic generation control. Email: shekharhimanshu33@gmail.com